

# Downlink RIS-NOMA with Constellation Adjustment for 6G Wireless Communication Systems

Ju Yeong Baek, Young-Seok Lee, and Bang Chul Jung

Dept. of Electronics Engineering, Chungnam National University, Daejeon 34134, Republic of Korea

Email: jybaek@o.cnu.ac.kr, yslee@o.cnu.ac.kr, bcjung@cnu.ac.kr

**Abstract**—We consider a downlink reconfigurable intelligent surfaces-based non-orthogonal multiple access technique with constellation adjustment (RIS-NOMA-CA) for 6G wireless communication systems. We mathematically analyze the bit-error-rate (BER) performance of the RIS-NOMA-CA technique assuming the optimal joint maximum likelihood (JML) detector at receivers. To the best of our knowledge, theoretical analysis of the downlink RIS-NOMA-CA technique has not been reported in the literature. We show that the RIS-NOMA-CA technique yields a better BER performance than the conventional RIS-NOMA technique without CA through computer simulations, and our analytical result matches well with simulation results.

**Index Terms**—Reconfigurable intelligent surface (RIS), non-orthogonal multiple access (NOMA), bit-error-rates (BER).

## I. INTRODUCTION

For 6G wireless communication systems, a reconfigurable intelligent surface (RIS) has emerged as a promising technology to cope with a severe propagation-loss due to obstacles between transmitter and receiver in high-frequency bands [1]. Several studies on application of the RIS to non-orthogonal multiple access (NOMA) technique have been conducted to improve quality of services (QoS) including spectral efficiency, fairness, connection capacity, energy efficiency, etc [2], [3]. In particular, a constellation adjustment (CA) technique was applied to *uplink* RIS-NOMA for improving the error performance in [3], but the CA has not been applied to downlink RIS-NOMA technique. Furthermore, a bit-error-rate (BER) performance of RIS-NOMA with CA has not been theoretically analyzed in both uplink and downlink.

In this paper, we consider a downlink RIS-NOMA system with CA and mathematically analyze the BER performance of the downlink RIS-NOMA with CA. We show that the RIS-NOMA with CA significantly outperforms the conventional RIS-NOMA without CA in terms of BER through extensive computer simulations.

## II. DOWNLINK RIS-NOMA WITH CA

Fig. 1 illustrates a downlink RIS-NOMA systems consisting of a single base station (BS) with a single antenna,  $M$  user equipments (UEs) with a single antenna, and a single RIS with  $N$  elements. We assume that  $N$  elements of the RIS are partitioned into  $M$  sub-surfaces and the  $i \in \{1, \dots, M\}$ -th subsurface with  $N_i$  elements supports the  $i$ -th UE. The term  $\mathbf{h}_i \in \mathbb{C}^{N_i}$  represents the wireless channel vector from the  $i$ -th subsurface to the BS. We define  $\mathbf{g}_{m,i} \in \mathbb{C}^{1 \times N_i}$  as the wireless channel vector from the  $i$ -th subsurface to the  $m \in$

This work was supported in part by the Institute for Information and communications Technology Promotion (IITP) through Augmented Beam-routing: Carom-MIMO funded by the Korea Government (MSIT) under Grant 2021-0-00486 and in part by the National Research Foundation of Korea (NRF) funded by the Korea Government (MSIT) under Grant NRF-2022R111A3073740.

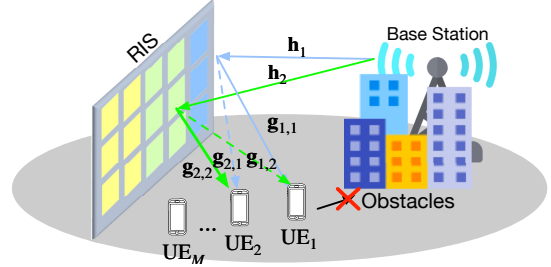


Fig. 1. System model of downlink RIS-NOMA with CA including a BS,  $M$  UEs, and an RIS with  $N$  elements.

$\{1, \dots, M\}$ -th UE. We assume that  $\mathbf{h}_i \sim \mathcal{CN}(\mathbf{0}, l_{\text{BR}}^\alpha \mathbf{I}_{N_i})$  and  $\mathbf{g}_{m,i} \sim \mathcal{CN}(\mathbf{0}, l_m^\alpha \mathbf{I}_{N_i})$  where  $l_{\text{BR}}$ ,  $l_m$  and  $\alpha$  denote the distance from the BS to the RIS, the distance from the  $m$ -th UE to the RIS, and the path-loss exponent, respectively. It is assumed that there exists no direct link between the BS and each UE. Let the  $n \in \{1, \dots, N_i\}$ -th element of  $\mathbf{h}_i$  and  $\mathbf{g}_{m,i}$  be  $h_{i,n}$  and  $g_{m,i,n}$ , respectively. The phase of each element is defined as  $\varphi_{i,n} := \angle h_{i,n}$  and  $\phi_{m,i,n} := \angle g_{m,i,n}$ . The phase shift coefficients of the  $i$ -th subsurface in the RIS can be represented with a diagonal matrix  $\mathbf{\Theta}_i \in \mathbb{C}^{N_i \times N_i}$  to maximize the received signal-to-noise ratio (SNR) at the  $i$ -th UE, where the  $n$ -th diagonal component of  $\mathbf{\Theta}_i$  is set to  $e^{-j(\varphi_{i,n} + \phi_{m,i,n})}$ . Then, the received signal at the  $m$ -th UE is given by

$$y_m = \sum_{i=1}^M \mathbf{g}_{m,i} \mathbf{\Theta}_i \mathbf{h}_i x + w_m, \quad (2)$$

where  $w_n$  denotes the additive noise, i.e.,  $w_m \sim \mathcal{CN}(0, \sigma^2)$  and  $x \in \mathbb{C}$  denotes the transmit signal of the BS. We consider the CA technique with QPSK modulation to improve the BER performance of the RIS-NOMA system. The term  $x$  represents the magnitude- and phase-adjusted weighted sum of QPSK symbols transmitted over NOMA, i.e.,  $\sum_{m=1}^M \sqrt{\tilde{a}_m P} s_m e^{j\delta_m}$ , where  $\delta_m$ ,  $\tilde{a}_m$ ,  $s_m$  and  $P$  represent angle of the steering phase, power allocation factor for  $m$ -th UE, normalized QPSK symbol for  $m$ -th UE, and transmit power, respectively [4]. The  $m$ -th UE tries to detect symbols  $\hat{\mathbf{s}} = [\hat{s}_1, \dots, \hat{s}_M]$  by utilizing the joint maximum likelihood (JML) detector as

$$\hat{\mathbf{s}} = \arg \min_{\mathbf{s}_1, \dots, \mathbf{s}_M \in \chi} \left| y_m - \sum_{i=1}^M \mathbf{g}_{m,i} \mathbf{\Theta}_i \mathbf{h}_i x \right|^2, \quad (3)$$

where  $\chi$  is a candidate set of normalized QPSK symbols, i.e.,  $\chi \triangleq \{c_1, c_2, c_3, c_4\} = \left\{ \frac{-1+j}{\sqrt{2}}, \frac{-1-j}{\sqrt{2}}, \frac{1+j}{\sqrt{2}}, \frac{1-j}{\sqrt{2}} \right\}$  [5].

## III. ERROR PERFORMANCE ANALYSIS

For the mathematical simplicity, we assume that the BS serves two UEs through the RIS in this section. Then, we denote a superimposed QPSK symbol as  $C_k = e^{j\delta_1} \sqrt{\tilde{a}_1} c_{[k/4]} +$

$$\Pr(\varepsilon_1) \leq \frac{1}{4} \sum_{p=1}^4 \sum_{q=5}^{16} \mathbb{E}_{\rho_1} \left[ e^{-t_1 \left( \rho_1 \sqrt{\frac{D_{p,q}^2 \gamma}{2}} \right)^2 - t_2 \left( \rho_1 \sqrt{\frac{D_{p,q}^2 \gamma}{2}} \right) - t_3} \right], \Pr(\varepsilon_2) \leq \frac{1}{4} \sum_{p=1}^4 \sum_{q \notin \mathcal{Q}_p} \mathbb{E}_{\rho_2} \left[ e^{-t_1 \left( \rho_2 \sqrt{\frac{D_{p,q}^2 \gamma}{2}} \right)^2 - t_2 \left( \rho_2 \sqrt{\frac{D_{p,q}^2 \gamma}{2}} \right) - t_3} \right], \quad (1)$$

$$\mathbb{E}_{\rho_m} \left[ e^{-t_1 \left( \rho_m \sqrt{\frac{D_{p,q}^2 \gamma}{2}} \right)^2 - t_2 \left( \rho_m \sqrt{\frac{D_{p,q}^2 \gamma}{2}} \right) - t_3} \right] = \frac{e^{-\frac{2t_3 v_m + \mu_m^2}{2v_m}} \cdot e^{\frac{(t_2 v_m D_{p,q} \sqrt{\gamma} - \sqrt{2} \mu_m)^2}{4t_1 v_m^2 D_{p,q}^2 \gamma + 4v_m}}}{2\sqrt{t_1 v_m D_{p,q}^2 \gamma + 1}} \left[ 1 + \operatorname{erf} \left( \sqrt{\frac{(t_2 v_m D_{p,q} \sqrt{\gamma} - \sqrt{2} \mu_m)^2}{4t_1 v_m^2 D_{p,q}^2 \gamma + 4v_m}} \right) \right].$$

$e^{j\delta_2} \sqrt{\tilde{a}_2} c_{((k-1) \bmod 4)+1}$ ,  $k \in \{1, 2, \dots, 16\}$  [4]. We exploit the optimal phase difference, i.e.,  $\delta_1 - \delta_2$ , and power allocation factor  $\tilde{a}$  which were derived in [3]. Assuming that the RIS has a large number of elements, an effective channel of the  $m$ -th UE,  $\psi_m = \sum_{i=1}^2 \mathbf{g}_{m,i} \mathbf{\Theta}_i \mathbf{h}_i$ , can be statistically modeled as the sum of non-central normal Gaussian and complex Gaussian distribution by central limit theorem [2]. Then, since phase shift coefficients of the RIS are designed to align phases of all wireless channels corresponding to each UE to maximize the received SNR, the real value of the effective channels containing the desired channel aligned by the RIS might be much larger than the imaginary value. Hence, an upper bound for the BER can be simply derived by reducing the channel amplitude of the effective channel  $|\psi_m|$  to the real part  $\Re\{\psi_m\}$ . For the ease of explanation, let  $\rho_m := \Re\{\psi_m\}$ . Then,  $\rho_m$  follows normal distribution where a mean of  $\mu_m$  and variance of  $v_m$  are derived as

$$\mu_m = N_m \sqrt{l_{\text{BR}}^\alpha l_m^\alpha} \frac{\pi}{4}, v_m = l_{\text{BR}}^\alpha l_m^\alpha \left\{ N_m \left( 1 - \frac{\pi}{16} \right) + \frac{(N - N_m)}{2} \right\}. \quad (4)$$

With the symmetry of QPSK constellations, we derive the error probability of the first UE when transmitting symbol  $c_1$  without loss of generality. Then, the union bound of the conditional BER given  $\rho_1$ , can be expressed as

$$\Pr(\varepsilon_1 | \rho_1) \leq \frac{1}{4} \sum_{p=1}^4 \sum_{q=5}^{16} Q \left( \rho_1 \sqrt{\frac{D_{p,q}^2 \gamma}{2}} \right), \quad (5)$$

where  $D_{p,q}$  denotes the Euclidean distance between superimposed constellation point  $C_p$  and  $C_q$  where  $(p, q \in \{1, 2, \dots, 16\})$  and  $\gamma := P/\sigma^2$ . Since (5) is mathematically intractable in deriving a closed form of the BER performance, we exploit a substitute of the  $Q$ -function which is known to be a tight approximation as  $Q(x) \approx e^{-t_1 x^2 - t_2 x - t_3}$  in [6] where  $t_1$ ,  $t_2$ , and  $t_3$  denote fitting parameters. Consequently, the upper bound of the BER of the RIS-NOMA with CA in the case of two UEs can be derived as (1) where  $\mathcal{Q}_p$  denotes an index set of constellations that do not cause errors from the perspective of the second UE when the BS transmits  $C_p$ .

#### IV. SIMULATION RESULTS

In this section, we validate the BER performance of downlink RIS-NOMA with CA through Monte-Carlo simulations and we verify analytical result on the BER of the presented system by comparing with the simulation result. For simulation setup, We set  $l_{\text{BR}}$  to 20m,  $l_1$  to 6m,  $l_2$  to 4m, the number of elements  $N$  in the RIS to 200, and the path loss exponent to 2. We consider an environment where two UEs exist, and the number of elements of a subsurface within the RIS to serve each UE is 100, i.e.,  $N_1 = N_2 = 100$ . Fig. 2 shows the

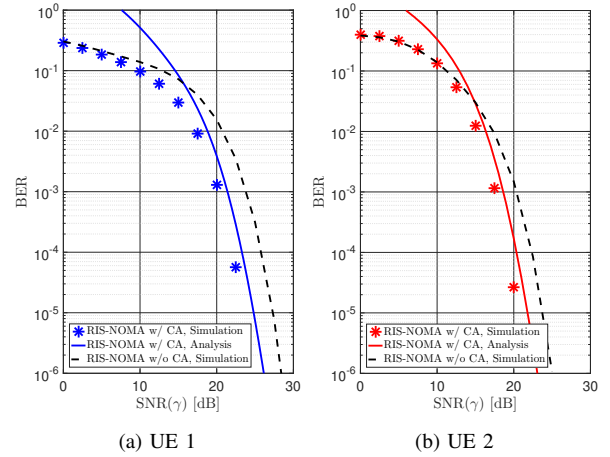


Fig. 2. BER performance of downlink RIS-NOMA with CA when  $N_1 = N_2 = 100$  and  $(l_{\text{BR}}, l_1, l_2) = (20\text{m}, 6\text{m}, 4\text{m})$ .

BER performance of downlink RIS-NOMA with CA technique for varying SNR at (a) UE 1 and (b) UE 2, respectively. It can be seen that applying CA can achieve significant BER performance improvement compared to the case where CA is not applied in the downlink RIS-NOMA system. In addition, it is worth noting that our mathematical analysis is matched well with the simulation result.

#### V. CONCLUSION

We presented a downlink RIS-NOMA with constellation adjustment technique including signal rotation and scaling. We also mathematically analyzed the BER performance of the presented system by utilizing the characteristics of RIS with a large number of elements. Through computer simulations, we confirmed that a significant BER performance improvement can be achieved via CA in downlink RIS-NOMA systems.

#### REFERENCES

- [1] C. Pan *et al.*, "Reconfigurable intelligent surfaces for 6G systems: Principles, applications, and research directions," *IEEE Commun. Mag.*, vol. 59, no. 6, pp. 14-20, Jun. 2021.
- [2] A. Chauhan, S. Ghosh, and A. Jaiswal, "RIS partition-assisted non-orthogonal multiple access (NOMA) and quadrature-NOMA with imperfect SIC," *IEEE Trans. Wireless Commun.*, vol. 22, no. 7, pp. 4371-4386, Jul. 2023.
- [3] B. Y. D. Rito, and K. H. Li, "SER-effective constellation scaling and rotation in STAR-RIS-assisted uplink NOMA," *IEEE Commun. Lett.*, vol. 27, no. 9, pp. 2506-2510, Sept. 2023.
- [4] K.-H. Lee, J. S. Yeom, J. Joung, and B. C. Jung, "Performance analysis of uplink NOMA with constellation-rotated STLC for IoT networks," *IEEE Open J. Commun. Soc.*, vol. 3, pp. 705-717, Apr. 2022.
- [5] J. S. Yeom, H. S. Jang, K. S. Ko, and B. C. Jung, "BER performance of uplink NOMA with joint maximum-likelihood detector," *IEEE Trans. Veh. Technol.*, vol. 68, no. 10, pp. 10295-10300, Oct. 2019.
- [6] M. López-Benítez, and F. Casadevall, "Versatile, accurate, and analytically tractable approximation for the Gaussian Q-function," *IEEE Trans. Wireless Commun.*, vol. 59, no. 4, pp. 917-922, Apr. 2011.